

Unified Source-Free Domain Adaptation

Song Tang, Wenxin Su, Mao Ye✉, Jianwei Zhang, and Xiatian Zhu✉

Abstract—In the pursuit of transferring a source model to a target domain without access to the source training data, Source-Free Domain Adaptation (SFDA) has been extensively explored across various scenarios, including Closed-set, Open-set, Partial-set, and Generalized settings. Existing methods, focusing on specific scenarios, not only address a limited subset of challenges but also necessitate prior knowledge of the target domain, significantly limiting their practical utility and deployability. In light of these considerations, we introduce a more practical yet challenging problem, termed *unified SFDA*, which comprehensively incorporates all specific scenarios in a unified manner. In this paper, we propose a novel approach *latent Causal factors discovery for unified SFDA* (CausalDA). In contrast to previous alternatives that emphasize learning the statistical description of reality, we formulate CausalDA from a causality perspective. The objective is to uncover the causal relationships between latent variables and model decisions, enhancing the reliability and robustness of the learned model against domain shifts. To integrate extensive world knowledge, we leverage a pre-trained vision-language model such as CLIP. This aids in the formation and discovery of latent causal factors in the absence of supervision in the variation of distribution and semantics, coupled with a newly designed information bottleneck with theoretical guarantees. Extensive experiments demonstrate that CausalDA can achieve new state-of-the-art results in distinct SFDA settings, as well as source-free out-of-distribution generalization. Our code and data are available at <https://github.com/tntek/source-free-domain-adaptation>.

Index Terms—Unified domain adaptation, source-free, statistical association, latent causal factors, information bottleneck.

1 INTRODUCTION

DUE to escalating demands for privacy and information protection in public security and commercial competition, well-annotated training data are recognized as crucial for varying purposes, requiring stringent access control. However, in practical scenarios, the use of a source model (pre-trained on the source domain) without access to the actual source data, referred to as Source-Free Domain Adaptation (SFDA) [1], has become more feasible. This approach involves the challenges posed by strict data access controls and emphasizes the adaptation of a pre-trained model to new domains without relying on the availability of the original source data.

SFDA has been explored across various scenarios, as summarized in Tab. 1. The most constrained scenario, termed *Closed-set*, assumes identical categories of interest in both the source and target domains, focusing on addressing covariate shift, such as domain-specific appearance distributions [2]. *Generalized SFDA* extends this by requiring the adapted model to perform well in both the source and target domains without forgetting the source domain [3]. Moving beyond the vanilla category identity constraint, *Open-set SFDA* [4]

TABLE 1: Summary of different SFDA settings. C_s/C_t : The category set of the source/target domain.

Setting	Covariate shift	Semantic shift	Anti-forgetting	Category
Closed-set	✓	✗	✗	$C_s = C_t$
Generalized	✓	✗	✓	$C_s = C_t$
Open-set	✓	✓	✗	$C_s \subset C_t$
Partial-set	✓	✓	✗	$C_s \supset C_t$
Unified (Ours)	✓	✓	✓	Any

considers the target domain with additional categories, while *Partial-set SFDA* [5] takes the opposite direction. Both scenarios require handling the additional challenge of semantic shift.

Typically, prevalent SFDA methods tend to concentrate on particular scenarios, tackling only a subset of challenges. For instance, SFDA-DE [6] focuses on Closed-set scenarios, SF-PGL [7] on Open-set scenarios, PSAT [8] on Generalized settings, and CRS [9] on Partial-set scenarios. Nevertheless, this approach significantly restricts their practical utility and deployability, given that we often possess limited prior knowledge about the target domain and minimal control or selection over its conditions.

To address the aforementioned limitation, this study introduces a more realistic yet challenging problem, referred to as *Unified Source-Free Domain Adaptation (Unified SFDA)*, with the goal of comprehensively addressing all the specific scenarios mentioned in a unified manner. To achieve this, we propose a novel approach *latent Causal discovery of salient factors for unified SFDA (CausalDA)*, going beyond conventional statistical association learning of related variables by exploring the underlying causal relationships [10]. The causal mechanism discovered is expected to be more reliable in varying distributions and semantic contexts, providing a unified solution for different scenarios of SFDA.

✉ Corresponding authors: Mao Ye, and Xiatian Zhu.

Song Tang is with the Institute of Machine Intelligence, University of Shanghai for Science and Technology, Shanghai, China; the TAMS Group, Department of Informatics, Universität Hamburg, Hamburg, Germany.

Wenxin Su is with the Institute of Machine Intelligence, University of Shanghai for Science and Technology, Shanghai, China.

Mao Ye is with the School of Computer Science and Engineering, University of Electronic Science and Technology of China, Chengdu, China.

Jianwei Zhang is with the TAMS Group, Department of Informatics, Universität Hamburg, Hamburg, Germany.

Xiatian Zhu is with the Surrey Institute for People-Centred Artificial Intelligence, and Centre for Vision, Speech and Signal Processing, University of Surrey, Guildford, UK.

Manuscript received April 19, 2022; revised August 26, 2022.

In the absence of label supervision for both distributional and semantic variations, our CausalDA is specifically formulated using a structural causal model in the logits space. The latent causal factors are disentangled into two complementary parts: (i) *external causal factors* and (ii) *internal causal factors*, consider that the information of both domains is not necessarily complete. For the former, we leverage a pre-trained large Vision-Language (ViL) model with rich knowledge such as CLIP [11], which has been exposed to a vast amount of multimodality information sources. The latter is identified under the guidance of discovered external causal factors. The discovery of external and internal causal factors is alternated by designing a self-supervised information bottleneck with theoretical guarantees.

Our **contributions** are summarized as follows:

- (i) For the first time, we introduce a unified SFDA problem that comprehensively incorporates various specific scenarios. This design eliminates the need for prior knowledge about the target domain before model deployment, enhancing practical usability and applicability in real-world scenarios.
- (ii) We introduce a novel approach for unified SFDA, termed CausalDA. Instead of learning the statistical description of the problem reality as conventional methods do, our CausalDA is formulated under the causality perspective. It aims to reveal the underlying causal relationships between latent variables and model decisions, providing favorable robustness against both distributional and semantic shifts.
- (iii) Extensive experiments demonstrate that CausalDA consistently achieves new state-of-the-art results on varying SFDA scenarios as well as source-free out-of-distribution generalization.

2 RELATED WORK

2.1 Source-free domain adaptation

Most of the prior SFDA methods consider the Closed-set setting where the source and target domains share the same classes, and the focus is on cross-domain distribution alignment. Existing methods exist in two categories. The first converts SFDA to Unsupervised Domain Adaptation (UDA) by constructing a pseudo-source domain [12], exploiting source prototype-guided data generation [13] or splitting source-like subset from target data [14]. The second follows the paradigm of self-supervised learning [15], [16], introducing self-guidance. Besides widely used pseudo-labels [15], [17], geometry information [18], [19], [20], contrastive data [9] and historical data [8] have also been exploited.

Recently, more practical settings have been studied. For example, the Generalized setting shifts aims to mitigate forgetting the source domain [3]. A representative approach is combining continual learning techniques with cross-domain adaptation, e.g., the domain attention-based gradient regulation [3] and source guidance constructed by historical information refining [8]. There exist works considering Open-set [7] and Partial-set [21] settings. For instance, to control the Open-set risk, a progressive balanced pseudo-labeling strategy [7] and Closed-set class prototypes are proposed [22]. Estimating the target data distribution helps with negative transfer reduction from the partial classes shift [23].

Alternatively, some works were proposed to enhance the discriminating ability for out-of-distribution classes [24]. There are two main strategies: Expanding inter-class distance to prevent semantic confusion [15], [25], and introducing external semantics, e.g., CLIP, to match out-of-distribution [26].

Most recently, multimodal large models such as CLIP and ShareGPT [27] have been introduced to advance SFDA, substantially enhancing adaptation performance by leveraging generic knowledge in these models. Two strategies are adopted: (1) customizing and adapting this knowledge via mutual knowledge distillation [28], [29] or multi-teacher guidance [30]; and (2) further denoising ViL predictions [31]. Critically, we highlight a couple of key aspects that make CausalDA conceptually distinct from these SFDA methods. First, CausalDA is unique in design philosophy by learning a causal representation, in contrast to the statistical knowledge DIFO [28] and ProDe [31] both are designed to learn. As a consequence, the outreach and generalization can be further extended, leading to the first dedicated unified SFDA approach. Instead, DIFO and ProDe predominantly focus on the conventional closed-set setting. Further, this conceptual discrepancy leads to distinct leveraging of ViL knowledge. DIFO and ProDe both employ the generic ViL knowledge directly as supervision, fostering the establishment of statistical relationships, whilst CausalDA utilizes ViL knowledge to uncover the underlying causal factors for capturing the essence of visual recognition.

Existing works as above focus on a specific SFDA setting, limiting their usability and generality substantially in practice. To address this limitation, we introduce a unified SFDA setting that incorporates all the pre-existing scenarios. With this new setup, we aim to foster more advanced SFDA methods that could generalize to a variety of problem settings without the need for designing and maintaining an array of distinct algorithms.

2.2 Causality methods in transfer learning

Causality methods aim for a robust function relation between random variables, which is insensitive to the extra variation/disturbing [32]. This property leads to recent popularity of this new paradigm in transfer learning, e.g., UDA [33], domain generalization (DG) [34], and out of distribution (OOD) [35]. These attempts aim to reduce non-causal factors by introducing artificial intervention. For example, the probability distribution change (used to represent the domain shift) and the semantic consistency constraint are jointly employed to implement this intervention. As source labels are available to ensure consistency, these methods emphasize constructing the distribution change in two lines. One explicitly generates augmented data to disturb the distribution, e.g., the non-linear augmentation and spatially-variable blending augmentation [36], inverse Fourier transformation augmentation [37], and generative models-based cross-domain image style transformation [38], [39]. The other implicitly modifies the distribution by exploiting cross-domain data. For example, MatchDG [40] developed cross-domain contrastive learning where the input's positive sample was randomly selected from samples with the same class. COR [35] adopted the variational inference encoder to infer unobserved causal factors from historical data, taking the time domain as a natural distribution change.

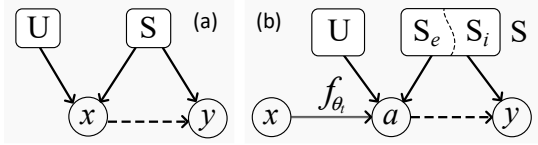


Fig. 1: Comparison of Structural Causal Models (SCM). (a) SCM for transfer learning with source domain, where S and U represent causal and non-causal factors. Domain shift is generally caused by U , which, together with the generalizable information S , e.g., the shape/structure of a dog (see Fig. 2), form the observation x . (b) Our proposed SCM for SFDA in a latent space (e.g., the logit a) where the causal factors S are decomposed into the external S_e and internal S_i components.

Compared with the existing works, the following three features distinguish CausalDA from them. (i) CausalDA does not rely on real labels that are indispensable for previous works. (ii) CausalDA discovers the causal factors instead of indirectly removing the non-causal ones. (iii) CausalDA builds the structural causal model at the logits level, whilst previous methods construct on raw data.

3 METHODOLOGY

3.1 Unified SFDA problem

SFDA aims to transfer a model pre-trained on the source domain to a different but related target domain without labeling. Formally, let $\mathcal{X}_s = \{\mathbf{x}_i^s\}_{i=1}^{n_s}$ and $\mathcal{Y}_s = \{y_i^s\}_{i=1}^{n_s}$ be the source samples and their truth labels. Similarly, the unlabeled samples and the truth target labels are $\mathcal{X} = \{\mathbf{x}_i\}_{i=1}^n$ and $\mathcal{Y} = \{y_i\}_{i=1}^n$, respectively. The unified SFDA task is to learn a target model $f_{\theta_t} : \mathcal{X} \rightarrow \mathcal{Y}$ without any prior knowledge of the target domain not the relationships between the source and target domains (see Tab. 1), given (i) the source model f_{θ_s} pre-trained over $\mathcal{X}_s, \mathcal{Y}_s$, and (ii) the unlabeled target data \mathcal{X} .

3.2 Causality in transfer learning with source domain

In transfer learning with available source domain, such as DG and UDA, the causality relation hidden in the statistical dependence (between raw image x and available label y) can be summarized to a Structural Causal Model (SCM). As depicted in Fig. 1(a), x is generated jointly by non-causal factors U and causal factors S , while label y is determined by S alone. Here, non-causal factors collectively represent the latent variables that generate the category-independent appearance of images, e.g., different domain styles and spurious dependence (Fig. 2); The causal factors present the ones determining the classification, e.g., the object shape.

In a causal view, solving the transfer learning involves eliminating the domain shift by building a robust classification function, i.e., $P(y|S)$. With SCM, we need to disconnect U to x . So existing works impose intervention upon x , according to the intervention theory [10]. Formally, this scheme can be formulated as

$$P(y|S) = P(y|do(x), S), \quad (1)$$

where $do(\cdot)$ means the do-operation of imposing intervention upon variables.

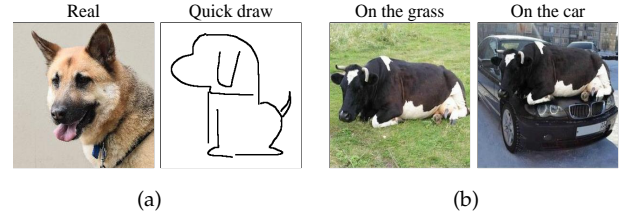


Fig. 2: Illustration of domain shift. (a) **Different appearance styles** of dog; (b) **Spurious dependence of background**: Cow in grass ground vs. on a car.

Approach	Intervention	Consistency
Existing [33], [34], [35]	Data augmentation	Supervised
CausalDA	Using logit	Unsupervised

TABLE 2: Analogy of causality learning.

In summary, the key idea is that when we change the probability distribution of non-causal factors (intervention) whilst keeping the category (prediction consistency), the causality can be extracted. Often, domain-related data augmentation is adopted as an intervention, whilst the source labels ensure prediction consistency. However, both conditions are unavailable in SFDA, making it inapplicable.

3.3 Latent causality in unified SFDA

To address the challenges outlined earlier, we propose an approach named *latent Causal factors discovery* (CausalDA), taking into account the following considerations. Instead of extracting causality in the raw input space x , we shift our focus to the logit space A : $a = f_{\theta_t}(x) \in A$. The choice of this space for causality analysis is crucial for two main reasons: First and foremost, from a causal perspective, using a post-intervened space enhances causality capture by incorporating a probability distribution shift into the data [10], [35], [40]. In our case, the logit space is post-intervened due to the inherent distribution shift between the in-training target model (initialized with the pre-trained source domain model) and the target domain. Specifically, the target model's logits for the target domain data reflect this domain shift, making them a particular form of post-intervention in this context.

Furthermore, the logit space is both highly semantic and compact, making it more efficient to manipulate. Since logits encode rich semantic information about class relationships, operating in this space allows for better generalization and transferability across domains. Additionally, its compact representation reduces computational complexity, facilitating more efficient learning and adaptation. These properties collectively make the logit space a more effective choice for our approach. Tab. 2 presents an analogy of CausalDA and the existing causal learning approach.

An overview of our proposed CausalDA framework is illustrated in Fig. 1(b). It models both non-causal factors U and causal factors S within a latent space A . Notably, the causal component S is further decomposed into internal (S_i) and external (S_e) sub-components to facilitate a more complete and interpretable modeling of causality.

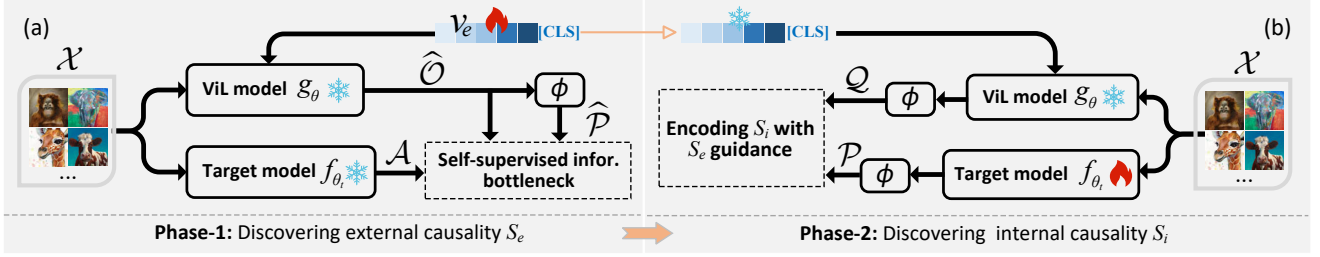


Fig. 3: Overview of our CausalDA framework: (a) Phase-1: Discovering the external causal factors S_e in form of prompt context v_e from a frozen ViL model using our self-supervised information bottleneck algorithm; (b) Phase-2: Discovering the internal causal factors S_i where the updated prompt context v_e is used to predict pseudo-labels as the prior information.

This internal-external causality decomposition is motivated by the recognition that identifying all relevant causal relationships solely from the source and target domains is often infeasible due to limited training data and domain-specific knowledge. To address this, we introduce a pre-trained ViL model, such as CLIP, as an external knowledge source to aid in the discovery of causal relationships. This design leads to two types of causality: (i) **Internal causality** referring to causal factors that can be inferred from the source domain model and the target domain data; (ii) **External causality**, additional complements captured from the ViL model with broad, many-domain information. Such a collaborative design enables a more holistic understanding of causal structures, as empirically validated in Sec. 4.6.1 and Sec. 4.6.3.

In contrast to conventional intervention-driven learning, we focus on discovering S from the intertwined S and U as

$$P(\mathbf{y}|S) = P(\mathbf{y}|\text{dis}(S|\{U, S\})), \quad S = \{S_i, S_e\}, \quad (2)$$

where $\text{dis}(S|\{U, S\})$ means conducting discover operation on $\{U, S\}$ to decompose S . To make this process computationally tractable, we consider

Principle 1. Independent Causal Mechanisms (ICM) Principle [41]: The conditional distribution of each variable given its causes (i.e., its mechanism) does not inform or influence the other mechanisms.

As discussed in Sec. 3.2, the lack of access to the source domain prevents the use of conventional causal learning methods. Inspired by Principle 1, we assume conditional independence between external and internal causal factors to enable a divide-and-conquer learning approach. Under this perspective, we propose the following factorized approximation as:

$$P(\mathbf{y}|S) \approx P(\mathbf{y}|\text{dis}(S_e|\{U, S_e\})) \cdot P(\mathbf{y}|\text{dis}(S_i|\{U, S_i\})). \quad (3)$$

3.4 CausalDA design

We present a concrete design to carry out CausalDA, as depicted in Fig. 3. By Eq. (3), we implement the causality discovery in two successive phases: phase-1 for S_e and phase-2 for S_i , as detailed below.

3.4.1 External causality discovery

To obtain external causality for a target task, we explore the potential of recent large multimodal ViL models such as CLIP [11]. This is because they have accumulated a vast amount of knowledge and exhibited strong generalization abilities across a wide range of perception tasks.

Specifically, we accomplish this idea by encoding S_e into the prompt context v_e of a ViL model g_θ efficiently. That is, our learning target is v_e , which is the explicit expression of S_e . We start by formulating the S_e discovery as maximizing the correlation between a random variable representing S_e and the prediction of the target model. Then, the original formulation is converted to a self-supervised information bottleneck problem with a theoretical guarantee, followed by the deep learning instantiation.

With the target samples \mathcal{X} and learnable v_e , we obtain the prediction of g_θ as $\hat{\mathcal{P}} = \{\hat{\mathbf{p}}_i\}_{i=1}^n$. Meanwhile, we obtain the logits of target model f_{θ_t} for the same data as $\mathcal{A} = \{\mathbf{a}_i\}_{i=1}^n$. We introduce three random variables, V , Y , and Z , following the probability distributions of v_e , $\hat{\mathcal{P}}$ and \mathcal{A} , respectively. In CausalDA, we further write

$$Z = \{Z_e, Z_i\} \quad (4)$$

where the latent random variables Z_e and Z_i represent the external S_e and the internal S_i causal factors, respectively.

In an information-theoretic view, for causality relationships, we have to ensure the correlation between Z_e and V . This could be considered an approximation with computational ease. Formally, discovering S_e needs maximizing the following mutual information:

$$\max_{v_e} I(Z_e, V), \quad (5)$$

where $I(\cdot, \cdot)$ is mutual information of two random variables. Note, mutual information is not a prerequisite for causality discovery; instead, it is an effective design choice that enhances the discovery of external causality.

To achieve Eq. (5), we employ prompt learning [42] to accomplish the optimization. This is because it allows us to leverage CLIP without tuning model parameters. This avoids potential issues such as catastrophic forgetting and unintended distortion of the pretrained knowledge within the ViL model. Moreover, by preserving CLIP's pretrained knowledge, prompt learning facilitates the discovery of external causality, enabling more effective integration of external knowledge into the causal learning process.

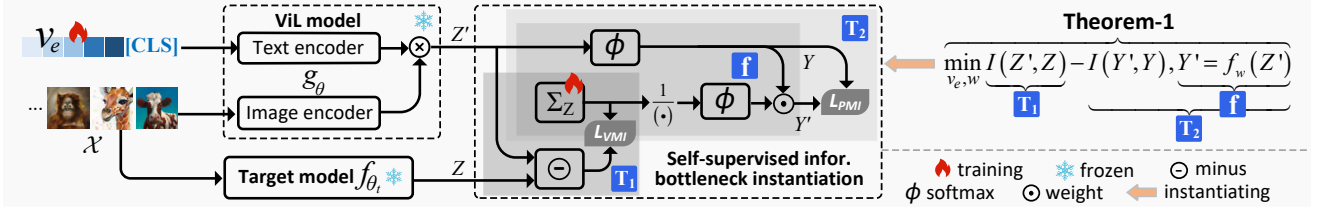


Fig. 4: Realizing our self-supervised information bottleneck w.r.t. **Theorem 1**. The item T_1 is estimated by Variational Mutual Information (VMI) with Gaussian distribution assumption $\mathcal{N}(Z, \Sigma_Z)$. The item T_2 is computed by Probabilistic Mutual Information (PMI) where the function f_w integrates the min-max optimization, using the covariance matrix Σ_Z from T_1 as the weighting parameters w .

Consider that prompt V is specific to the ViL model g_θ , we further transform the above formula of Eq. (5) as

$$\max_{v_e} I(Z_e, Y), Y = \phi(g_\theta(V)), \quad (6)$$

where $\phi(\cdot)$ is softmax function; so that the two variables under correlation maximization reside in similar semantic spaces. Theoretically, we prove that this transformation can constitute a lower bound on the original, ensuring its validity in optimization.

First, we have the following **Lemma 1** (see the proof in Appendix-A).

Lemma 1. Given random variables Z_1, X_1 and Y_1 where X_1, Y_1 satisfy a mapping $f_1 : X_1 \mapsto Y_1$. When f_1 is compressed, i.e., the output's dimension is smaller than the input's,

$$I(Z_1, X_1) \geq I(Z_1, Y_1). \quad (7)$$

The ViL model g_θ is indeed compressing, as it maps a high-dimensional image to a low-dimensional category vector. Let $Z_1 = Z_e, X_1 = X, Y_1 = Y$ and $f_1 = \phi(g_\theta(\cdot))$, we have $I(Z_e, V) \geq I(Z_e, Y)$ according to **Lemma 1**.

Self-supervised information bottleneck. In Eq. (6), Z_e is the hidden part of the observable logits along with non-causal and internal causal factors. To facilitate this learning process of Z_e , we derive a self-supervised information bottleneck algorithm without prior assumption on the distribution [43]. In general, information bottleneck conducts min-max optimization to squeeze out the essentials w.r.t. a task. We introduce a random variable Z' (i.e., the bottleneck) for the ViL's logits $\hat{O} = \{\hat{o}_i\}_{i=1}^n$ between V and Y , thereby forming a bottleneck style expression as:

$$\min_{v_e} I(Z, Z') - I(Z', Y), \quad (8)$$

where Z is the logit variable of target model f_{θ_t} which is observed. Note, we do not include the item $I(Z', Y)$ in minimization due to lacking supervision signal like ground-truth labels as used in conventional information bottleneck [44], i.e., a self-supervised formulation. However, we theoretically prove that Eq. (8) admits an upper bound, thus optimizationally valid.

Theorem 1. Suppose that there are five random variables Z, V, Z', Y and Y' . Among them, Z represents the target domain knowledge; V, Z' and Y express the input instances, an intermediate features of the ViL model and predictions, respectively; Y' depicts a pseudo-label that has a functional

relationship f_w (w is learnable parameters) with Z' . When f_w is reversible and uncompressed, we have this upper bound:

$$\begin{aligned} & \min_{v_e} I(Z, Z') - I(Z', Y) \\ & \leq \min_{v_e, w} \underbrace{I(Z, Z') - I(Z', Y)}_{T_1} \underbrace{I(Y', Y)}_{T_2}, \quad (9) \end{aligned}$$

The proof is given in Appendix-B. **Theorem 1** suggests that the desired latent factors refinement is conditionally equivalent to a self-supervised information bottleneck, when pseudo-label Y' is generated from the intermediate ViL feature Z' without information loss.

We realize the proposed information bottleneck using variational information maximization [45]. The key is to construct the function f_w with three properties: (i) The output is a probability distribution, e.g., including a softmax operation ϕ . (ii) No information loss, e.g., no zero weights in w for weighting-based functions. (iii) The weighting parameters w are constrained to be relevant to $I(Z', Z)$. The instantiations of T_1 and T_2 are elaborated below.

As exactly computing mutual information of two vector variables is intractable, we maximize the variational lower bound for the term T_1 (see the proof in [46]):

$$\begin{aligned} I(Z, Z') &= \mathbb{E}_{Z, Z'} \left[\log \frac{q(Z'|Z)}{p(Z')} \right] + \text{KL}(q(Z'|Z) \| p(Z'|Z)) \\ &\geq H(Z') + \mathbb{E}_{Z, Z'} (\log q(Z'|Z)), \end{aligned} \quad (10)$$

where $q(Z'|Z)$ is variational distribution approximating the real distribution $p(Z'|Z)$, $\text{KL}(\cdot, \cdot)$ is KL-divergence function, and $H(Z')$ is a constant. In practice, we model $q(Z'|Z)$ as a Gaussian distribution $\mathcal{N}(Z, \Sigma_Z)$ with mean Z and diagonal covariance matrix Σ_Z . For minimizing T_1 , we adopt the Variational Mutual Information (VMI) loss (see T_1 in Fig. 4):

$$\begin{aligned} \mathcal{L}_{\text{VMI}}(\mathcal{X}; v_e, \Sigma_Z) &= -\mathbb{E}_{Z, Z'} \left(\|Z' - Z\|_{\Sigma_Z^{-1}}^2 + \log |\Sigma_Z| \right) \\ &= -\frac{1}{n} \sum_{i=1}^n (\hat{o}_i - \mathbf{a}_i)^T \Sigma_Z^{-1} (\hat{o}_i - \mathbf{a}_i) + \log |\Sigma_Z|. \end{aligned} \quad (11)$$

Consider that the ViL's prediction Y and the pseudo-label Y' are probability distributions, we compute the T_2 term by vanilla mutual information [47]: $I(Z, Z') =$

$p(Z, Z')/[p(Z)p(Z')]$. The corresponding Probabilistic Mutual Information (PMI) loss function is formed as:

$$\mathcal{L}_{\text{PMI}}(\mathcal{X}; \mathbf{v}_e, \Sigma_Z) = \frac{1}{n} \sum_{i=1}^n I(\hat{\mathbf{p}}_i, \mathbf{p}'_i), \quad (12)$$

with $\hat{\mathbf{p}}_i = \phi(\hat{\mathbf{o}}_i)$, $\mathbf{p}'_i = f_w(\hat{\mathbf{o}}_i)$,

where $\sum_{c=1}^C \mathbf{p}'_{i,c} = 1$; $f_w(\cdot)$ is a weighting-based function constructed as follows.

From Eq. (11), $I(Z', Z)$ is a Mean-Square Error (MSE) weighted by Σ_Z . That means Σ_Z detects dimension importance duration minimization, with high-weight dimensions to be suppressed, thus corresponding to the non-causal factors U in our formulation. Thus, taking $1/\Sigma_Z$ as the weighting parameters of f_w shifts the focus of predicting to the causal component S_e (see **f** in Fig. 4), formally,

$$\mathbf{p}'_i = f_{[w=\Sigma_Z^i]}(\hat{\mathbf{o}}_i) = \phi\left(\phi\left(\frac{1}{\Sigma_Z^i}\right) \odot \phi(\hat{\mathbf{o}}_i)\right), \quad (13)$$

where $\phi(\cdot)$ is softmax function. Combining Eq. (11), (12), and (13) together, our self-supervised objective for external causality discovery is formed as

$$\begin{aligned} \min_{\mathbf{v}_e, \Sigma_Z} \mathcal{L}_{\text{EC}}(\mathcal{X}; \mathbf{v}_e, \Sigma_Z) \\ = \mathcal{L}_{\text{PMI}}(\mathcal{X}; \mathbf{v}_e, \Sigma_Z) - \alpha \mathcal{L}_{\text{VMI}}(\mathcal{X}; \mathbf{v}_e, \Sigma_Z). \end{aligned} \quad (14)$$

Remark. Our design differs from the existing information bottleneck in two aspects: While previous information extraction [48] is confined to a single model, ours is a cross-model design. Our formulation is self-supervised, in contrast to previous supervised designs.

3.4.2 Internal causality discovery

In phase-2, we subsequently discover the internal causal factors S_i by updating the target model. That is, we encode S_i in the target model, as it is latent in nature. Similar to capturing the external factors S_e (Eq. (5)), this encoding can be formulated by maximizing the following conditional mutual information:

$$\max_{\theta_t} I(Z_i, Z_\theta), \quad \text{s.t.} \quad \max_{\theta_t} I(Z_e^*, Z_\theta) \quad (15)$$

where the random variable Z_θ represents target model parameters θ_t , whilst Z_i denotes the random variable of internal causal factors S_i (Eq. (4)); Z_e^* represents the currently discovered external causal factor S_e^* . The primary term, $\max_{\theta_t} I(Z_i, Z_\theta)$, aims to capture the internal causality S_i . The condition, $\max_{\theta_t} I(Z_e^*, Z_\theta)$, ensures the target model simultaneously accommodates the discovered external causality S_e^* .

Given ultra-high dimension and complexity of θ_t , combined with the hidden nature of Z_i , directly optimizing or computing Eq. (15) is intractable. To address this, we interpret the interaction between Z_θ and Z_i as the inherent modeling process that transforms an input sample from pixel space into a predictive probability space. This perspective allows us to reformulate the problem as maximizing the mutual information between the target model's input and output, both of which are *observed* and *operational*. Crucially, theoretical proofs demonstrate that mutual information between inputs and outputs is maximized when outputs are both highly confident and exhibit balanced class distributions

Algorithm 1 Training CausalDA

Input: Unlabelled target data \mathcal{X} , pre-trained source model f_{θ_s} , a frozen ViL model g_θ , max training iteration number M , prompt context \mathbf{v}_e .

- 1: Initialize the target model f_{θ_t} by f_{θ_s}
- 2: Initialize \mathbf{v}_e with a fixed template
- 3: **for** iter $k = 1$ to M **do**
- 4: Sample a mini-batch \mathcal{X}_b from \mathcal{X} .
- 5: Discover external causal factors S_e : update (\mathbf{v}_e, Σ_Z) by optimizing $\mathcal{L}_{\text{EC}}(\mathcal{X}_b; \mathbf{v}_e, \Sigma_Z)$, fixing \mathcal{L}_{IC} .
- 6: Convert updated \mathbf{v}_e to target pseudo-labels for this batch \mathcal{X}_b , i.e., obtain $\mathcal{Q}_b = \phi(g_\theta(\mathcal{X}_b, \mathbf{v}_e))$.
- 7: Discover internal causal factors S_i : update f_{θ_t} by optimizing \mathcal{L}_{IC} , fixing \mathcal{L}_{EC} .
- 8: **end for**
- 9: **return:** The adapted model f_{θ_t} .

[49]. Inspired by this theoretical finding, we maximize this originally non-computable mutual information by minimizing the following objective:

$$\mathcal{L}_{\text{UN}}(\mathcal{P}; \theta_t) = - \sum_{i=1}^n \mathbf{p}_i \log \mathbf{p}_i + \tau \sum_{c=1}^C \text{KL}\left(\mathcal{Q}_c \parallel \frac{1}{C}\right), \quad (16)$$

with $\mathbf{p}_i \in \mathcal{P} = \phi(f_{\theta_t}(\mathcal{X}))$.

In this equation, \mathcal{P} represents the predictions of n training samples \mathcal{X} generated by the target model f_{θ_t} . The first term minimizes the information entropy of each prediction $\mathbf{p}_i = [p_{i,c}]_{c=1}^C$. The KL divergence term, on the other hand, regulates the predictive balance across all C categories via pulling the empirical distribution $\mathcal{Q}_c = \frac{1}{n} \sum_{i=1}^n p_{i,c}$ towards a uniform distribution. The trade-off parameter τ balances these two terms.

Similarly, we convert the external causality S_e^* from its prompt format \mathbf{v}_e to pseudo-labels by evaluating the ViL model g_θ : $\mathcal{Q} = \phi(g_\theta(\mathcal{X}, \mathbf{v}_e))$. This conversion simplifies model optimization, as it enables the use of the conventional softmax cross-entropy loss, $\mathcal{L}_{\text{SCE}}(\mathcal{P}, \mathcal{Q}; \theta_t)$.

Combining these elements, we optimize Eq. (15) using the following objective function:

$$\mathcal{L}_{\text{IC}} = \min_{\theta_t} \mathcal{L}_{\text{UN}}(\mathcal{P}; \theta_t) + \sigma \mathcal{L}_{\text{SCE}}(\mathcal{P}, \mathcal{Q}; \theta_t) \quad (17)$$

where σ serves as another trade-off parameter.

3.5 Model training

We train CausalDA in an alternating manner. In each iteration, we first optimize prompt context \mathbf{v}_e with \mathcal{L}_{EC} whilst the target model is frozen (i.e., phase-1), followed by training the target model by \mathcal{L}_{IC} (i.e., phase-2) while the prompt context is frozen. The ViL model is always frozen throughout. More details for training are presented in Alg. 1.

4 EXPERIMENTS

4.1 Implementation details

Source models. Following [42], for source-free out-of-distribution generalization (SF-OODG) we adopt the Pytorch built-in ResNet50 model (pre-trained on ImageNet) as the

TABLE 3: Closed-set results (%) on **Office-Home**, **VisDA**. SF and ViL means source-free and ViL model-required, respectively.

Method	Venue	SF	ViL	Office-Home														VisDA
				Ar→Cl	Ar→Pr	Ar→Rw	Cl→Ar	Cl→Pr	Cl→Rw	Pr→Ar	Pr→Cl	Pr→Rw	Rw→Ar	Rw→Cl	Rw→Pr	Avg.	Sy→Re.	
Source	–	–	–	43.7	67.0	73.9	49.9	60.1	62.5	51.7	40.9	72.6	64.2	46.3	78.1	59.2	49.2	
CLIP-RN [11]	ICML21	–	✓	51.9	81.5	82.5	72.5	81.5	82.5	72.5	51.9	82.5	72.5	51.9	81.5	72.1	83.7	
CLIP-B32 [11]	ICML21	–	✓	59.8	84.3	85.5	74.6	84.3	85.5	74.6	59.8	85.5	74.6	59.8	84.3	76.1	82.9	
DAPL-RN [50]	TNNLS23	✗	✓	54.1	84.3	84.8	74.4	83.7	85.0	74.5	54.6	84.8	75.2	54.7	83.8	74.5	86.9	
PADCLIP-RN [51]	ICCV23	✗	✓	57.5	84.0	83.8	77.8	85.5	84.7	76.3	59.2	85.4	78.1	60.2	86.7	76.6	88.5	
ADCLIP-RN [52]	ICCV23W	✗	✓	55.4	85.2	85.6	76.1	85.8	86.2	76.7	56.1	85.4	76.8	56.1	85.5	75.9	87.7	
SHOT [15]	ICML20	✓	✗	55.0	78.7	81.3	69.1	78.9	79.1	68.2	53.6	81.6	73.5	59.4	83.5	71.8	82.9	
GKD [25]	IROS21	✓	✗	56.5	78.3	82.2	69.2	80.4	78.7	67.4	55.4	82.6	74.3	60.3	84.2	72.5	83.0	
NRC [18]	NeurIPS21	✓	✗	57.2	79.3	81.3	68.9	80.6	80.2	66.6	57.3	82.0	71.0	57.9	84.9	72.3	85.9	
AaD [53]	NeurIPS22	✓	✗	59.3	79.3	82.1	68.9	79.8	79.5	67.2	57.4	83.1	72.1	58.5	85.4	72.7	88.0	
AdaCon [54]	CVPR22	✓	✗	47.2	75.1	75.5	60.7	73.3	73.2	60.2	45.2	76.6	65.6	48.3	79.1	65.0	86.8	
CoWA [23]	ICML22	✓	✗	57.3	79.3	81.0	69.3	77.9	79.6	68.1	56.4	82.6	72.9	61.3	83.7	72.4	86.9	
PLUE [17]	CVPR23	✓	✗	49.1	73.5	78.2	62.9	73.5	74.5	62.2	48.3	78.6	68.6	51.8	81.5	66.9	88.3	
TPDS [55]	IJCV24	✓	✗	59.3	80.3	82.1	70.6	79.4	80.9	69.8	56.8	82.1	74.5	61.2	85.3	73.5	87.6	
SHOT-B32 [15]	ICML20	✓	✓	64.7	84.0	86.4	79.4	87.3	85.4	78.1	65.8	87.6	81.6	65.0	88.5	79.5	85.2	
GKD-B32 [25]	IROS21	✓	✓	67.2	83.2	84.3	77.0	84.8	83.6	75.5	71.1	86.0	81.1	72.4	88.5	79.6	85.3	
NRC-B32 [18]	NeurIPS21	✓	✓	55.0	83.4	86.7	78.3	86.5	85.1	77.1	69.9	87.2	90.9	65.5	88.4	79.5	88.2	
AaD-B32 [53]	NeurIPS22	✓	✓	69.4	83.0	84.9	76.4	85.2	84.6	73.3	71.1	86.3	79.0	72.1	88.7	79.5	82.6	
TPDS-B32 [55]	IJCV24	✓	✓	67.7	82.7	86.1	76.5	88.0	86.3	73.6	69.4	87.1	79.3	70.5	89.7	79.7	78.0	
CausalDA-C-RN	–	–	✓	60.1	85.6	86.2	77.2	86.0	86.3	76.6	61.0	86.5	77.5	61.4	86.2	77.6	89.3	
CausalDA-C-B32	–	–	✓	72.3	89.8	89.9	81.1	90.3	89.5	80.1	71.5	89.8	81.8	72.7	90.4	83.3	89.3	

TABLE 4: Closed-set results (%) on **DomainNet-126**. SF and ViL means source-free and ViL model-required, respectively.

Method	Venue	SF	ViL	C→P	C→R	C→S	P→C	P→R	P→S	R→C	R→P	R→S	S→C	S→P	S→R	Avg.
Source	–	–	–	44.6	59.8	47.5	53.3	75.3	46.2	55.3	62.7	46.4	55.1	50.7	59.5	54.7
CLIP-RN [11]	ICML21	–	✓	70.2	87.1	65.4	67.9	87.1	65.4	67.9	70.2	65.4	67.9	70.2	87.1	72.7
CLIP-B32 [11]	ICML21	–	✓	73.5	85.7	71.2	74.7	85.7	71.2	74.7	73.5	71.2	74.7	73.5	85.7	76.3
DAPL-RN [50]	TNNLS23	✗	✓	72.4	87.6	65.9	72.7	87.6	65.6	73.2	72.4	66.2	73.8	72.9	87.8	74.8
ADCLIP-RN [52]	ICCV23W	✗	✓	71.7	88.1	66.0	73.2	86.9	65.2	73.6	73.0	68.4	72.3	74.2	89.3	75.2
SHOT [15]	ICML20	✓	✗	63.5	78.2	59.5	67.9	81.3	61.7	67.7	67.6	57.8	70.2	64.0	78.0	68.1
GKD [25]	IROS21	✓	✗	61.4	77.4	60.3	69.6	81.4	63.2	68.3	68.4	59.5	71.5	65.2	77.6	68.7
NRC [18]	NeurIPS21	✓	✗	62.6	77.1	58.3	62.9	81.3	60.7	64.7	69.4	58.7	69.4	65.8	78.7	67.5
AdaCon [54]	CVPR22	✓	✗	60.8	74.8	55.9	62.2	78.3	58.2	63.1	68.1	55.6	67.1	66.0	75.4	65.4
CoWA [23]	ICML22	✓	✗	64.6	80.6	60.6	66.2	79.8	60.8	69.0	67.2	60.0	69.0	65.8	79.9	68.6
PLUE [17]	CVPR23	✓	✗	59.8	74.0	56.0	61.6	78.5	57.9	61.6	65.9	53.8	67.5	64.3	76.0	64.7
TPDS [55]	IJCV24	✓	✗	62.9	77.1	59.8	65.6	79.0	61.5	66.4	67.0	58.2	68.6	64.3	75.3	67.1
SHOT-B32 [15]	ICML20	✓	✓	72.8	84.5	72.0	75.1	85.2	72.2	78.2	75.5	71.6	75.2	73.6	83.2	76.6
GKD-B32 [25]	IROS21	✓	✓	73.7	84.4	73.6	76.1	85.4	73.6	80.4	76.9	73.9	74.9	74.8	82.1	77.5
NRC-B32 [18]	NeurIPS21	✓	✓	72.2	83.4	72.5	75.1	84.8	72.6	78.3	76.7	74.0	75.0	73.7	82.6	76.7
AaD-B32 [53]	NeurIPS22	✓	✓	72.2	84.2	72.0	75.3	85.3	72.6	78.2	77.4	73.6	74.8	74.7	82.8	76.9
TPDS-B32 [55]	IJCV24	✓	✓	72.5	82.8	71.8	77.7	84.7	72.9	81.9	76.5	72.8	73.5	74.2	83.0	77.0
CausalDA-C-RN	–	–	✓	75.4	88.2	72.0	75.8	88.3	72.1	76.1	75.6	71.2	77.6	75.9	88.2	78.0
CausalDA-C-B32	–	–	✓	77.2	88.0	75.2	78.8	88.2	75.8	79.1	77.8	74.9	79.9	77.4	88.0	80.0

source model, taking ImageNet variations as evaluation datasets. For all the other settings, the source model is trained on the source domain in a supervised manner, same as [15], [18], [20].

Networks. Our CausalDA involves two parts: the ViL model and the target model. We choose CLIP [11] as the ViL model. The target model’s structure is the same as the source model. Following [15], [19], a target model consists of a feature extractor and a classifier (an FC layer). We adapt the feature extractor, which is pre-trained on ImageNet. For fair comparison, we use ResNet101 as the backbone for VisDA and ResNet50 for the others.

Training. There are three parameters with CausalDA: α in L_{EC} (Eq. (14)), τ in L_{UN} (Eq. (16)), and σ in L_{IC} (Eq. (17)). For all settings, we adopt the same configuration $(\alpha, \sigma, \tau) = (0.003, 0.4, 1.0)$. Here, since the value of \mathcal{L}_{VMI} is large, α is set as small as 0.003. For model training, we use a batch size of 64, an SGD optimizer with momentum 0.9, and 15 epochs on all datasets. The learnable prompt template is initialized with ‘a photo of a [CLS].’ [11], where the [CLS] means a specific target class name.

4.2 Closed-set SFDA

Datasets. We evaluate CausalDA on three challenging benchmarks. **Office-Home** [56] is a middle-scale dataset. It contains 15k images belonging to 65 categories from working or family environments, being divided into four domains, i.e., **Artistic images**, **Clip Art**, **Product images**, and **Real-word images**. **VisDA** [57] is a large-scale dataset. It includes 12 types of **Synthetic to Real** transfer recognition tasks. The source domain contains 152k synthetic images, whilst the target domain has 55k real object images from COCO. **DomainNet-126** [58] is another large-scale dataset. As a subset of DomainNet containing 600k images of 345 classes from 6 domains of different image styles, this dataset has 145k images from 126 classes, sampled from 4 domains, **Clipart**, **Painting**, **Real**, **Sketch**, as [58] identifies severe noisy labels in the dataset.

Competitors. To evaluate CausalDA, we select 14 state-of-the-art methods in three groups. (i) *The first* is the source model and CLIP that lay the basis for CausalDA. (ii) *The second* is the UDA method DAPL [50], PADCLIP [51], ADCLIP [52] that introduces prompt learning to boost the cross-

TABLE 5: One step adapting results (%) on **Office-Home** in Generalized SFDA setting. S, T, H are the results on the source and target domains, and harmonic mean accuracy, respectively; the bracket values in red are the gap between S and T; WAD means With Anti-forgetting Design.

Method	Venue	WAD	Avg.		
			S	T	H
Source	–	✗	98.1	59.2	73.1
SHOT [15]	ICML20	✗	84.2	71.8	77.1
GKD [25]	IROS21	✗	86.8	72.5	78.7
NRC [18]	NeurIPS21	✗	91.3	72.3	80.4
AdaCon [54]	CVPR22	✗	88.2	65.0	74.4
CoWA [23]	ICML22	✗	91.8	72.4	80.6
PLUE [17]	CVPR23	✗	96.3	66.9	78.4
TPDS [55]	IJCV24	✗	83.8	73.5	78.0
GDA [3]	ICCV21	✓	80.0	70.2	74.4
PSAT-RN [8]	TMM24	✓	85.3	72.6	78.4
SHOT-B32 [15]	ICML20	✗	81.9	79.5	80.7
GKD-B32 [25]	IROS21	✗	89.2	79.5	84.1
NRC-B32 [18]	NeurIPS21	✗	81.1	78.6	79.8
TPDS-B32 [55]	IJCV24	✗	88.9	79.7	84.1
PSAT-B32 [8]	TMM24	✓	89.5	80.7	84.9
CausalDA-C-RN	–	✗	85.0	77.6	80.7
CausalDA-C-B32	–	✗	86.3	83.3	84.5

domain transfer. (iii) *The third* includes 9 SFDA methods: SHOT [15], GKD [25], NRC [18], AaD [53], AdaCon [54], CoWA [23], PLUE [17], TPDS [55]. By idea, SHOT, GKD, CoWA are pseudo-labels-based methods; NRC, AaD, PLUE, AdaCon exploit the data geometry, e.g., the nearest neighbor, neighborhood, prototypes; and TPDS predicts the target probability distribution using error control.

For comprehensive comparisons, we implement two variants: (i) CausalDA-C-RN (base) and (ii) CausalDA-C-B32 (premium). The key distinction lies in the backbone of the CLIP image encoder. Specifically, for CausalDA-C-RN, ResNet101 is employed on the VisDA dataset, while ResNet50 is used on the Office-Home and DomainNet-126 datasets. On the other hand, CausalDA-C-B32 adopts ViT-B/32 [59] as the backbone across all datasets. This extends to all other methods using CLIP.

For an SFDA-focused comparison, we integrate the same CLIP model with existing SFDA methods, utilizing the CLIP’s visual backbone (ViT B/32) as the feature extractor, followed by the original training algorithm. As such, all compared methods benefit from the CLIP pre-trained knowledge in a design-generic manner. Specifically, we select five updated SFDA methods as comparisons, including SHOT-B32, GKD-B32, NRC-B32, AaD-B32, and TPDS-B32.

Results. The quantitative comparisons are listed in Tab. 3~4. Our CausalDA-C-RN and CausalDA-C-B32 perform best on all tasks across the three datasets. Compared with previous best SFDA methods TPDS (on Office-Home), PLUE (on VisDA) and GKD (on DomainNet-126), CausalDA-C-RN improves by 4.1%, 1.0% and 9.3% in average accuracy, respectively. Compared with these UDA methods with both access to labelled source data and CLIP, CausalDA-C-RN still improves by 1.0%, 0.8%, and 2.8% on top of second-best methods PADCLIP-RN (on Office-Home, VisDA) and ADCLIP-RN (on DomainNet-126). The improvement expands further when we switch focus to the strong version CausalDA-C-B32. Such results are unsurprising since the well-pretrained CLIP is employed to identify the external causal elements.

On the other hand, CausalDA-C-RN defeats CLIP-RN on all tasks, achieving the improvement of 4.5%, 5.6%, and 5.3% on Office-Home, VisDA, and DomainNet-126 on average, respectively. Similarly, compared with CLIP-B32, the corresponding improvement of CausalDA-C-B32 are changed to 7.2%, 6.4% and 3.7%. This indicates the effect of the prompt learning to discover the external causal elements.

Among the “-B32” models, we have two observations. First, CausalDA-C-B32 outperforms all conventional methods across all tasks on the three datasets, confirming the effectiveness of our design. Second, on the VisDA dataset, improvements with the B32 versions are limited, and they are even outperformed by the ResNet version, such as AaD and TPDS. This is because the rendered synthetic data (the source domain in VisDA) lacks visual details, appearing primarily in shades of white and gray light and shadow. When processed in ViT, this results in confused semantics. As for AaD and TPDS, contrastive computation (AaD) and chain-like search (TPDS) amplify the noise in the confused semantics, leading to uncontrolled error propagation.

4.3 Generalized SFDA

Dataset. We evaluate CausalDA on Office-Home, following previous Generalized SFDA works [3], [8].

Evaluation protocol. Unlike Closed-set SFDA, the Generalized SFDA problem highlights the anti-forgetting ability on the seen source domain. In terms of evaluation rule, the same as [3], we adopt the harmonic mean accuracy that is computed by $H = (2 * A_s * A_t) / (A_s + A_t)$ where A_s and A_t are the accuracy on the source domain and the target domain, respectively. Note that the A_s is computed based on the source-testing set. The same as [3], [8], on the source domain, the ratio of training and testing sets is 9:1.

Competitors. As listed in Tab. 5, two Generalized SFDA methods, GDA [3] and PSAT [8], are additionally selected for comparison. In GDA, domain attention was integrated with a local clustering-based self-supervised learning method. Essentially, knowledge about old tasks is kept by encouraging model parameters to be close to the original values. Instead, PSAT enforces the adaptation process to remember the source domain by imposing source guidance, building a target domain-centric anti-forgetting mechanism. As CausalDA, we make two PSAT variants with ResNet50 (PSAT-RN) and ViT (PSAT-B32).

One step adapting comparison. Tab. 5 reports the results, including source and target domain accuracies and their average. Among the “-B32” methods, CausalDA-C-B32 (without any anti-forgetting design) is only defeated by the best specially designed model PSAT-B32 (with anti-forgetting mechanism) with a gap of 0.4%. CausalDA-C-RN outperforms other alternatives with the same backbone. These results verify the competitiveness of our models in one-step adaptation.

Continual adapting results. We conduct continual adaptation testing following [3]. In the adaptation sequence $Ar \rightarrow Cl \rightarrow Pr \rightarrow Rw$, we first train an initial model on domain Ar, which then serves as the source for adaptation to domain Cl. This process repeats iteratively until the final adaptation to domain Rw is achieved, resulting in four distinct models. Each model is evaluated across all domains, with 10% of the data in each domain randomly selected as the test set.

TABLE 6: Continual adaptation results (%) on **Office-Home** under Generalized SFDA setting, the first column of each sub-table indicates the adaptation sequence. ↓ means the average accuracy drop of a test domain on the adaptation path compared with the performance when the domain is first seen.

CausalDA-C-RN																			
Test					Test					Test					Test				
	Ar	Cl	Pr	Rw		Cl	Ar	Pr	Rw		Pr	Ar	Cl	Rw		Rw	Ar	Cl	Pr
Ar	97.8	46.1	68.4	71.1	Cl	97.5	52.5	65.8	61.5	Pr	99.6	52.2	40.8	71.3	Rw	98.1	63.1	46.3	78.5
Cl	80.0	63.5	64.3	66.0	Ar	80.1	77.8	70.7	75.6	Ar	91.2	78.4	50.2	78.3	Ar	93.4	78.4	50.4	75.6
Pr	78.4	61.7	85.0	76.2	Pr	75.4	74.4	86.9	78.1	Cl	81.5	71.9	61.5	69.9	Cl	83.0	74.7	62.1	69.7
Rw	83.1	60.2	83.2	84.4	Rw	67.6	78.4	85.4	85.6	Rw	87.3	76.9	59.2	85.6	Pr	87.3	72.5	61.5	85.2
↓	17.3	2.5	1.8	–	↓	23.1	1.4	1.6	–	↓	13.0	4.1	2.3	–	↓	10.2	4.8	0.6	–

CausalDA-C-B32																			
Test					Test					Test					Test				
	Ar	Cl	Pr	Rw		Cl	Ar	Pr	Rw		Pr	Ar	Cl	Rw		Rw	Ar	Cl	Pr
Ar	97.8	46.1	68.4	71.1	Cl	97.5	52.5	65.8	61.5	Pr	99.6	52.2	40.8	71.3	Rw	98.1	63.1	46.3	78.5
Cl	84.1	77.0	69.3	72.5	Ar	80.9	83.4	72.3	77.0	Ar	90.0	82.5	49.4	80.1	Ar	94.0	82.8	51.2	76.8
Pr	82.5	70.9	91.0	81.1	Pr	74.2	78.1	90.4	82.2	Cl	83.6	75.6	76.2	76.2	Cl	85.2	73.8	76.2	72.5
Rw	86.3	67.6	88.3	87.7	Rw	69.5	81.3	88.9	89.1	Rw	89.8	79.1	69.5	87.7	Pr	89.5	76.9	71.5	90.0
↓	13.5	7.7	2.7	–	↓	22.6	3.7	1.5	–	↓	11.8	5.2	6.7	–	↓	8.5	7.5	4.7	–

TABLE 7: Partial-set, Open-set results (%) on **Office-Home**.

Partial-set SFDA			Open-set SFDA		
Method	Venue	Avg.	Method	Venue	Avg.
Source	–	62.8	Source	–	46.6
SHOT [15]	ICML20	79.3	SHOT [15]	ICML20	72.8
HCL [60]	NeurIPS21	79.6	HCL [60]	NeurIPS21	72.6
CoWA [23]	ICML22	83.2	CoWA [23]	ICML22	73.2
AaD [53]	NeurIPS22	79.7	AaD [53]	NeurIPS22	71.8
CRS [9]	CVPR23	80.6	CRS [9]	CVPR23	73.2
SHOT-B32 [15]	ICML20	80.6	SHOT-B32 [15]	ICML20	73.3
AaD-B32 [53]	NeurIPS22	81.2	AaD-B32 [53]	NeurIPS22	72.4
CausalDA-C-RN	–	82.9	CausalDA-C-RN	–	79.6
CausalDA-C-B32	–	85.8	CausalDA-C-B32	–	83.4

Tab. 6 presents the results of CausalDA-C-RN and CausalDA-C-B32. We highlight two observations with CausalDA-C-B32: **First**, if a domain has been encountered during continual adaptation, the adapted model does not degrade significantly on that domain. For example, in the adaptation sequence $Cl \rightarrow Ar \rightarrow Pr \rightarrow Rw$, when adapting from Cl to Ar, the accuracy on Ar reaches **83.4%**. Subsequent adaptations to Pr and Rw lead to an average performance drop of **3.7%** (see the second column in the second sub-table). **Second**, the adapted model performs well even on unseen domains. For instance, along the adaptation path $Ar \rightarrow Cl \rightarrow Pr \rightarrow Rw$, the model’s accuracy on Rw gradually improves from **71.1%** to **87.7%** (see the fifth column in the first sub-table). These results suggest that CausalDA effectively captures causal factors, making it robust to domain shifts.

4.4 Open-set & Partial-set SFDA

Dataset. We adopt Office-Home for evaluation [9], [15].

Competitors. Except Source, CLIP, SHOT, and CoWA as in the Closed-set setting, we consider two more contrastive learning based SFDA methods, HCL [60] and CRS [9].

Comparison results. As presented in Tab. 7, in terms of average accuracy, CausalDA-C-B32 surpasses not only all competitors with an improvement of **2.6%** and **10.2%** over CoWA (Partial-set) and CRS (Open-set). Similarly, it significantly outperforms SHOT-B32 and AaD-B32 under both Partial-set and Open-set settings, indicating the efficacy of the proposed design. Only CoWA beats CausalDA-C-RN in the Partial-set setting with a tiny lead **0.3%**. The results indicate that CausalDA is competitive for the Partial-set and Open-set settings.

TABLE 8: SF-ODG results (%) on **ImageNet variants**. L, ViL means label-required, ViL model-required, respectively.

Method	Venue	L	ViL	ImageNet \rightarrow X				
				IN-V2	IN-K	IN-A	IN-R	Avg.
Source	–	–	–	62.7	22.2	0.7	35.1	30.2
CLIP-RN [11]	ICML21	–	✓	51.5	33.3	21.8	56.1	40.7
CLIP-B32 [11]	ICML21	–	✓	54.8	40.8	29.5	66.2	47.8
CoOP-RN [42]	IJCV21	✓	✓	55.4	34.7	23.1	56.6	42.4
CoOP-B32 [42]	IJCV21	✓	✓	58.2	41.5	31.3	65.8	49.2
CoCoOp-RN [61]	CVPR22	✓	✓	55.7	34.5	23.3	57.7	42.8
CoCoOp-B32 [61]	CVPR22	✓	✓	56.6	40.7	30.3	64.1	47.9
TPT-RN [26]	NeurIPS22	✓	✓	54.7	35.1	26.7	59.1	43.9
ProGrad-RN [62]	ICCV23	✓	✓	54.7	34.4	23.1	56.8	42.2
ProGrad-B32 [62]	ICCV24	✓	✓	57.4	41.7	31.9	66.5	49.4
SHOT [15]	ICML20	✗	✗	62.5	38.4	2.1	42.7	36.4
GKD [25]	IROS21	✗	✗	62.3	38.2	2.1	42.2	36.2
NRC [18]	NeurIPS21	✗	✗	61.5	0.9	1.3	28.9	23.1
AdaCon [54]	CVPR22	✗	✗	50.9	18.5	2.0	38.6	27.5
CoWA [23]	ICML22	✗	✗	62.7	37.8	1.7	46.3	37.1
PLUE [17]	CVPR23	✗	✗	53.0	18.5	2.0	38.6	28.0
TPDS [55]	IJCV24	✗	✗	62.9	35.0	2.9	48.4	37.3
SHOT-B32 [15]	ICML20	✗	✓	69.4	43.6	1.6	58.2	43.2
GKD-B32 [25]	IROS21	✗	✓	53.5	45.2	1.0	58.3	39.5
NRC-B32 [18]	NeurIPS21	✗	✓	66.2	18.6	15.4	38.0	34.6
TPDS-B32 [55]	IJCV24	✗	✓	69.0	38.9	0.6	58.7	41.8
CausalDA-C-RN	–	✗	✓	64.4	42.6	22.3	61.5	47.7
CausalDA-C-B32	–	✗	✓	64.7	48.4	30.6	71.0	53.7

4.5 Source-free out-of-distribution generalization

Datasets. We evaluate CausalDA in the SF-ODG setting on four challenging **ImageNet Variants**. Specifically, **IN-V2** (i.e., ImageNet-V2) [63] is an independent set consisting of natural images, collected from different sources, a total of 10k images of 1000 ImageNet categories. **IN-A** (i.e., ImageNet-A) [64] is a challenging set consisting of these “natural adversarial examples” (misclassified by a vanilla ResNet50 [65]), containing 7.5k images of 200 ImageNet categories. **IN-R** (i.e., ImageNet-R) [66] is an ImageNet sub-set with artistic renditions. It contains 30k images covering 200 ImageNet categories. **IN-K** (i.e., ImageNet-Sketch) [67] collects black and white sketches from the ImageNet validation set. This dataset contains 50k images from 1000 ImageNet categories.

Competitors. In addition to the methods compared in the Closed-set SFDA setting, we include four more: CoOP [42], CoCoOp [61], TPT [26], and ProGrad [62]. Among them, CoOP, CoCoOp, and ProGrad employ prompt learning with supervision from a few labeled samples, while TPT introduces self-supervised prompt tuning by minimizing multi-view entropy.

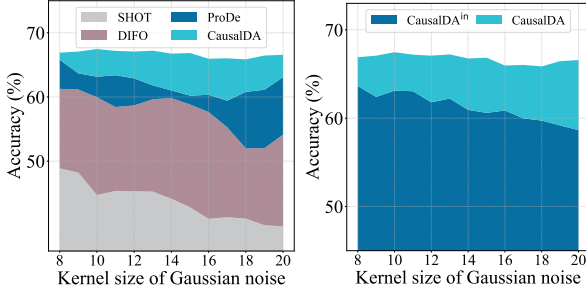


Fig. 5: Causality validation: Invariance analysis across varying noise settings on the Ar→Cl task of **Office-home**.

Comparison results. Tab. 8 reports the SF-OODG results. In average accuracy, our methods, CausalDA-C-NR and CausalDA-C-B32, outperform previous SFDA methods by a significant margin, achieving at least a 10% improvement. Even compared to CLIP and other CLIP-based methods, CausalDA maintains a clear advantage. For example, CausalDA-C-NR improves upon CLIP-C-RN by 7.0% and surpasses the second-best CLIP-based method, TPT-RN, by 3.8%. Among the “-B32” models, CausalDA-C-B32 excels with a margin of at least 10.5% over previous methods.

4.6 Further analysis

For all the following experiments, we use the strong variant of CausalDA, i.e., CausalDA-C-B32. For brevity, we remove the suffix ‘-C-B32’.

4.6.1 Validation of causal factors

Validating the discovery of causal factors is significant yet non-trivial in causality learning, especially with latent causal factors as in this study. To that end, we adopt a general principle that there exists an intimate connection between invariance and causality useful for generalization [32], [68]. That being said, if a learned model enables varying environments generalization, it is then indicated that causal predictors have been captured (e.g., causal explanation of an object such as why it is a computer).

Concretely, we simulate a spectrum of viewing environments by imposing varying levels of Gaussian noise with gradually increased kernel sizes from 8 to 20. We compare the competitors without (SHOT [15]) and with (DIFO [28] and ProDe [31]) ViL knowledge. As shown in Fig. 5, all competitors degrade clearly as the noise increases, whilst CausalDA levels off. This validates that our method has uniquely captured the underlying invariant predictors to make our model causal. To further examine if external and internal factors both are effective, we further derive a variant of CausalDA, named as CausalDAⁱⁿ, without the external causality discovery. Specifically, in CausalDAⁱⁿ, the pseudo-labels are directly derived from CLIP’s zero-shot predictions. It is evident that external factors are useful in improving the invariance ability, confirming its complementarity with the internal counterparts.

4.6.2 Causal vs. statistical SFDA

In this strategic evaluation, we contrast CausalDA with two state-of-the-art statistical SFDA methods, DIFO [28] and

ProDe [31], both of which are equipped with the same ViL model. Our analysis focuses on two critical modeling aspects, examined across various SFDA settings: *Domain fitness*: Evaluated under Closed-set conditions; *Domain generalization*: Assessed across Generalized, Partial-set, Open-set, and SF-OODG settings.

Based on this evaluation, we draw the following key observations: (1) Domain fitness (Closed-set SFDA): As presented in Tab. 9, CausalDA is indeed outperformed by both DIFO and ProDe in the Closed-set setting. This is attributed to the inherent statistical learning nature of these alternatives, which tends to overfit their models towards the specific target domain. (2) Under the Generalized SFDA setting, CausalDA demonstrates significantly superior performance compared to DIFO. While achieving similar harmonic mean accuracy to ProDe, CausalDA exhibits the least drop in source domain accuracy. This suggests that ViL denoising is a crucial factor, conceptually orthogonal to our causality learning approach, contributing significantly to performance in this setting. (3) Broad domain generalization across the Open-set, Partial-set, and SF-OODG settings, CausalDA consistently stands out with strong performance. This highlights the superior domain generalization capabilities achieved through our method’s causal knowledge discovery. Importantly, our approach provides the best overall solution across all these diverse settings. Collectively, these results validate that our approach strikes the optimal balance between domain fitness and generalization, thereby laying a solid foundation to serve as a unified SFDA solution.

4.6.3 Analysis for causal factors discovery

We conduct causality analysis in two aspects: (1) complementarity of internal and external causality, and (2) analysis for the discovery process based on pseudo-label.

Complementarity of internal and external causality.

As aforementioned, causal factors originate from both the domain data itself (encoded internal causality) and external knowledge sources (encoded external causality). To illustrate this complementarity, we conduct an intuitive empirical experiment on the target domain. Specifically, we fuse the zero-shot predictions of the source model (Source) and a ViL model like CLIP using a logical OR operation. That is, if either CLIP or Source correctly predicts the true category of an input instance x , we consider x correctly classified. As shown in Fig. 6, Fusion-OR significantly outperforms both Source and CLIP individually, reinforcing the plausibility of our internal-external causality partition.

Pseudo-label-based analysis for discovery process.

In CausalDA, the external causal elements S_e are identified and converted into pseudo-labels. Thus, the quality of these pseudo-labels serves as an indicator of the discovery process. To evaluate this, we compare pseudo-label-based methods SHOT, COWA, and GKD, along with CLIP’s zero-shot predictions (denoted as CLIP). The results, shown in Fig. 7, demonstrate that CausalDA-PL achieves significantly higher pseudo-label accuracy than prior methods, benefiting from CLIP-assisted S_e discovery. Furthermore, the performance curve of CausalDA remains consistently above that of CausalDA-PL, with a significant gap throughout training. This highlights the effectiveness of capturing internal causal elements S_i , further enhancing model performance.

TABLE 9: Causal vs. statistical SFDA. OH/VDA/DN126: **Office-Home/VisDA/DomainNet-126**. S/T: Source/Target domain; H : Harmonic mean accuracy; H_{all} : Average over all settings (H metric used for Generalized SFDA). H_g : Average over all settings except closed-set.

Method	Venue	Closed-set				Generalized			Open-set	Partial-set	SF-ODG					H_{all}
		OH	VDA	DN126	Avg.	S	T	H	T	T	IN-V2	IN-K	IN-A	IN-R	Avg.	H_g
Source	–	59.2	49.2	54.7	54.4	98.1	59.2	73.8	46.6	62.8	62.7	22.2	0.7	35.1	30.2	53.4
DIFO [28]	CVPR24	83.1	90.3	80.0	84.5	78.0	83.1	80.5	75.9	85.6	59.6	37.7	25.2	66.4	47.2	72.3
ProDe [31]	ICLR25	84.5	91.0	85.0	86.8	85.1	84.5	84.8	82.6	84.2	62.1	45.8	24.7	69.7	50.6	75.5
CausalDA	–	83.3	89.3	80.0	84.2	86.3	83.3	84.5	83.4	85.8	64.7	48.4	30.6	71.0	53.7	76.9

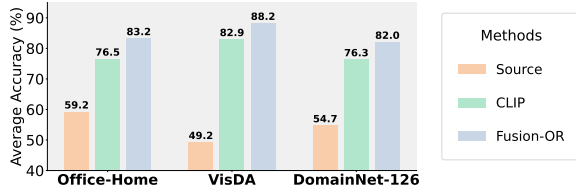


Fig. 6: Zero-shot fusion results (Fusion-OR) of CLIP and the source model (Source) under the Closed-set SFDA setting on the **Office-Home**, **VisDA**, and **DomainNet-126** datasets. This fusion method follows the logical OR principle: An input instance is considered correctly classified if either CLIP or the source model predicts its ground truth category.

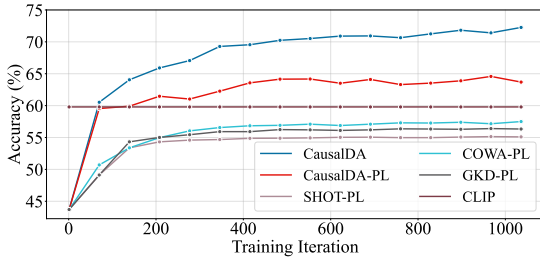


Fig. 7: Accuracy change of pseudo-label during training on the Ar→Cl task of **Office-home**.

4.6.4 Model analysis

Feature distribution visualization. Feature distribution provides an intuitive way to evaluate classification performance. We compare five methods: The source model (Source), CLIP, SHOT, TPDS, and Oracle (trained on domain Cl with real labels). Fig. 8 presents the logit visualization results using a 3D density chart. As we move from Source to CausalDA, the clustering effect progressively improves, with CausalDA exhibiting the most structured distribution, closely resembling Oracle.

Ablation study. In CausalDA, we separately discover the causal factors $S = \{S_e, S_i\}$. To isolate the effect of this strategy, we evaluate four variations: (i) CausalDA-w- S_i : We use only \mathcal{L}_{UN} from Eq. (17) as the objective for model training, allowing us to assess the impact of capturing S_i . (ii) CausalDA-w- S_e : We apply pseudo-label supervised learning, regulated by \mathcal{L}_{SCE} , where the pseudo-labels are generated from S_e discovery, regulated by L_{EC} . This isolates the effect of capturing S_e . (iii) CausalDA-w-CLIP: We directly use CLIP’s zero-shot results as pseudo-labels to regulate the discovery of S_i . (iv) CausalDA-w-P1: We retain only the

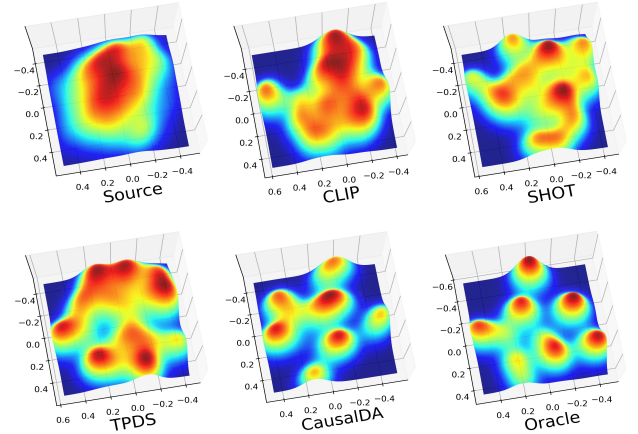


Fig. 8: Logit distribution visualization on transfer task Ar→Cl in the **Office-Home** dataset. Oracle: model trained on the real labels of domain Cl. For a clear view, the first ten categories are displayed.

TABLE 10: Ablation study results (%). CS, OS, PS, and GS mean the Closed-set, Open-set, Partial-set, and Generalized SFDA settings, respectively.

Method	Office-Home				Avg.	IN-K
	CS	OS	PS	GS		
Source	59.2	46.6	62.8	73.1	60.4	30.2
CausalDA-w-S_i	70.3	71.5	70.1	75.9	72.6	36.9
CausalDA-w-S_e	81.6	80.7	84.1	84.3	82.2	44.2
CausalDA-w-CLIP	80.9	78.3	83.9	82.5	80.6	44.2
CausalDA-w-P1	79.3	37.3	79.3	77.2	68.3	40.8
CausalDA	83.3	83.4	85.8	84.5	83.7	48.4

phase-1 objective, removing the loss \mathcal{L}_{IC} from Eq. (17).

Tab. 10 presents the results of these methods across four SFDA settings and SF-ODG. Specifically, both CausalDA-w- S_e and CausalDA-w- S_i outperform the Source model, but fall significantly behind the full CausalDA version. This suggests that capturing either S_e or S_i independently is effective, but both are necessary for optimal performance. The comparison between CausalDA-w-CLIP and CausalDA highlights the importance of L_{EC} -based prompt learning for S_e discovery. Finally, CausalDA-w-P1 performs considerably worse than CausalDA, emphasizing the value of our two-stage design in the causal factor capture pipeline.

Scalability study of IC instantiation. The objective \mathcal{L}_{IC} in Eq. (17), which regulates S_i discovery, is a component with multiple implementation options. To evaluate its scalability, we present three alternative instantiations for the two regula-

TABLE 11: Scalability study (%) of IC instantiation.

Loss	Method	Closed-set		SF-ODG
		Office-Home	VisDA	IN-K
\mathcal{L}_{UN}	CausalDA+ENT	82.5	89.4	46.8
	CausalDA+NRC	83.0	87.9	47.5
	CausalDA+TPDS	83.5	90.2	45.0
\mathcal{L}_{SCE}	CausalDA+ $\ \cdot\ _1$	82.3	88.2	44.9
	CausalDA+ $\ \cdot\ _2$	82.8	88.2	40.3
	CausalDA+KL	83.5	89.1	49.1
CausalDA		83.3	89.2	48.4

TABLE 12: Prompt initialization study (%).

# Initialization template	Closed-set		SF-ODG
	Office-Home	VisDA	IN-K
1 'X [CLASS].' (#X=4)	82.6	89.1	48.4
2 'X [CLASS].' (#X=16)	81.5	88.5	46.1
3 'There is a [CLASS].'	83.6	89.2	48.6
4 'This is a photo of a [CLS].'	83.7	89.0	48.8
5 'This is maybe a photo of a [CLS].'	83.0	89.1	48.8
6 'This is almost a photo of a [CLS].'	83.7	89.2	48.4
7 'This is definitely a photo of a [CLS].'	83.5	88.9	48.1
8 'a picture of a [CLS].'	83.5	88.8	48.6
9 'a photo of a [CLS].'	83.3	89.2	48.4

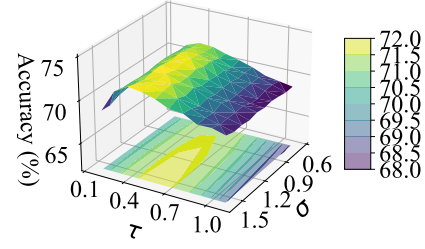
tors in \mathcal{L}_{IC} . For \mathcal{L}_{UN} , we consider the following alternatives: (i) CausalDA+ENT: Entropy regularization without category balance constraints, (ii) CausalDA+NRC: Data local structure-based regularization, (iii) CausalDA+TPDS: Domain shift control-based regularization. For \mathcal{L}_{SCE} , we test three popular methods: 1-Norm ($\|\cdot\|_1$), 2-Norm ($\|\cdot\|_2$), and KL Divergence.

As shown in Tab. 11, in the Closed-set setting, CausalDA+TPDS achieves the best results, with other methods lagging by up to 2%. This indicates that these typical regulators do not significantly affect model performance in this setting. In the SF-ODG setting, all methods (except CausalDA+KL) show a slight accuracy drop compared to CausalDA. For CausalDA+ENT, removing the category balance regularization leads to a performance decrease. The performance loss for CausalDA+NRC and CausalDA+TPDS is attributed to the fact that these methods do not specifically address the SF-ODG setting.

For \mathcal{L}_{SCE} , the results show that probability distribution approximation (KL Divergence) outperforms feature-based methods ($\|\cdot\|_1$ and $\|\cdot\|_2$) in preserving model performance in the presence of external causal elements.

Effect of prompt initialization. In CausalDA, we employ prompt learning to encode the external causal factors S_e . Here, we examine four different prompt initialization strategies (Tab. 12): (i) the conventional constant strategy (rows 1–2), (ii) the sentence strategy (rows 3–4), (iii) the uncertainty strategy (rows 5–7), and (iv) an innovative approach of sentence initialization with different phrase (rows 8–9), which considers the lack of precise supervision in SFDA.

Tab. 12 shows the comparison results for these nine templates across both the Closed-set setting and SF-ODG. The results indicate that the different templates do not cause significant performance differences, suggesting that CausalDA is relatively insensitive to prompt selection. However, when comparing the constant strategy to the others, it becomes clear that initializing with semantic information is the more effective option, which aligns with our expectations.

Fig. 9: Parameter sensitiveness study (σ, τ) on transfer task Ar→Cl in Office-Home.

Parameters sensitiveness. Taking the transfer task Ar→Cl in Office-Home for example, we evaluate the sensitivity of CausalDA by varying the hyper-parameters $0.2 \leq \sigma \leq 1.1$, $0.7 \leq \tau \leq 1.6$ at the step of 0.1. Fig. 9 indicates that both corresponding terms matter, whilst their sensitivity to performance is not high.

5 CONCLUSION

We introduce a more challenging Unified SFDA problem that comprehensively addresses all specific scenarios within a unified framework. To tackle this, we propose CausalDA, a novel approach grounded in causality, fundamentally differing from previous methods based on statistical dependence. Specifically, we design a self-supervised information bottleneck to capture external causal elements, convert them into pseudo-labels, and use them to guide the discovery of internal causal factors. Building on our theoretical insights, we implement this information bottleneck using a network-based variational mutual information approach. Extensive experiments across various SFDA settings and SF-ODG validate the superiority of CausalDA over existing methods.

Acknowledgments

This work is partially supported by the National Natural Science Foundation of China (NSFC) (62476169, 62206168, 62276048); the German Research Foundation and NSFC in project Crossmodal Learning under contract Sonderforschungsbereich Transregio 169, the Hamburg Landesforschungsförderungsprojekt Cross, NSFC (61773083); Horizon2020 RISE project STEP2DYNA (691154).

REFERENCES

- [1] Y. Kim, D. Cho, K. Han, P. Panda, and S. Hong, "Domain adaptation without source data," *IEEE Trans. on Artif. Intell.*, vol. 2, no. 6, pp. 508–518, 2021.
- [2] R. Li, Q. Jiao, W. Cao, H.-S. Wong, and S. Wu, "Model adaptation: Unsupervised domain adaptation without source data," in *Proc. IEEE Conf. Comput. Vis. Pattern Recog. (CVPR)*, 2020, pp. 9641–9650.
- [3] S. Yang, Y. Wang, J. Van De Weijer, L. Herranz, and S. Jui, "Generalized source-free domain adaptation," in *Proc. IEEE Int. Conf. Comput. Vis. (ICCV)*, 2021, pp. 8978–8987.
- [4] P. Panareda Busto and J. Gall, "Open set domain adaptation," in *Proc. IEEE Int. Conf. Comput. Vis. (ICCV)*, 2017, pp. 754–763.
- [5] Z. Cao, K. You, M. Long, J. Wang, and Q. Yang, "Learning to transfer examples for partial domain adaptation," in *Proc. IEEE Conf. Comput. Vis. Pattern Recog. (CVPR)*, 2019, pp. 2985–2994.
- [6] N. Ding, Y. Xu, Y. Tang, C. Xu, Y. Wang, and D. Tao, "Source-free domain adaptation via distribution estimation," in *Proc. IEEE Conf. Comput. Vis. Pattern Recog. (CVPR)*, 2022, pp. 7212–7222.

- [7] Y. Luo, Z. Wang, Z. Chen, Z. Huang, and M. Baktashmotlagh, "Source-free progressive graph learning for open-set domain adaptation," *IEEE Trans. Pattern Anal. Mach. Intell.*, 2023.
- [8] S. Tang, Y. Shi, Z. Song, M. Ye, C. Zhang, and J. Zhang, "Progressive source-aware transformer for generalized source-free domain adaptation," *IEEE Trans. on Multimedia*, vol. 26, pp. 4138–4152, 2024.
- [9] Y. Zhang, Z. Wang, and W. He, "Class relationship embedded learning for source-free unsupervised domain adaptation," in *Proc. IEEE Conf. Comput. Vis. Pattern Recog. (CVPR)*, 2023, pp. 7619–7629.
- [10] J. Pearl, *Causality*. Cambridge university press, 2009.
- [11] A. Radford, J. W. Kim, C. Hallacy, A. Ramesh, G. Goh, S. Agarwal, G. Sastry, A. Askell, P. Mishkin, J. Clark, et al., "Learning transferable visual models from natural language supervision," in *Proc. Int. Conf. Mach. Learn. (ICML)*. PmlR, 2021, pp. 8748–8763.
- [12] R. Li, Q. Jiao, W. Cao, H. Wong, and S. Wu, "Model adaptation: Unsupervised domain adaptation without source data," in *Proc. IEEE Conf. Comput. Vis. Pattern Recog. (CVPR)*, 2020, pp. 9638–9647.
- [13] J. Tian, J. Zhang, W. Li, and D. Xu, "VDM-DA: Virtual domain modeling for source data-free domain adaptation," *IEEE Trans. Circuits Syst. Video Technol.*, vol. 32, no. 6, pp. 3749–3760, 2021.
- [14] Y. Du, H. Yang, M. Chen, J. Jiang, H. Luo, and C. Wang, "Generation, augmentation, and alignment: A pseudo-source domain based method for source-free domain adaptation," *Mach. Learn.*, vol. 113, pp. 3611–3631, 2024.
- [15] J. Liang, D. Hu, and J. Feng, "Do we really need to access the source data? source hypothesis transfer for unsupervised domain adaptation," in *Proceedings of the Int. Conf. Mach. Learn. (ICML)*, 2020, pp. 6028–6039.
- [16] W. Chen, L. Lin, S. Yang, D. Xie, S. Pu, and Y. Zhuang, "Self-supervised noisy label learning for source-free unsupervised domain adaptation," in *Proc. IEEE Int. Intell. Rob. Syst. (IROS)*. IEEE, 2022, pp. 10 185–10 192.
- [17] M. Litrico, A. Del Bue, and P. Morerio, "Guiding pseudo-labels with uncertainty estimation for test-time adaptation," in *Proc. IEEE Conf. Comput. Vis. Pattern Recog. (CVPR)*, 2023.
- [18] S. Yang, J. van de Weijer, L. Herranz, S. Jui, et al., "Exploiting the intrinsic neighborhood structure for source-free domain adaptation," *Proc. Adv. Neural Inform. Process. Syst. (NeurIPS)*, vol. 34, pp. 29 393–29 405, 2021.
- [19] S. Yang, Y. Wang, J. van de Weijer, L. Herranz, S. Jui, and J. Yang, "Trust your good friends: Source-free domain adaptation by reciprocal neighborhood clustering," *IEEE Trans. Pattern Anal. Mach. Intell.*, 2023.
- [20] S. Tang, Y. Zou, Z. Song, J. Lyu, L. Chen, M. Ye, S. Zhong, and J. Zhang, "Semantic consistency learning on manifold for source data-free unsupervised domain adaptation," *Neural Networks*, vol. 152, pp. 467–478, 2022.
- [21] W. Li and S. Chen, "Partial domain adaptation without domain alignment," *IEEE Trans. Pattern Anal. Mach. Intell.*, vol. 45, no. 7, pp. 8787–8797, 2023.
- [22] G. Vray, D. Tomar, B. Bozorgtabar, and J.-P. Thiran, "Distill-SODA: Distilling self-supervised vision transformer for source-free open-set domain adaptation in computational pathology," *IEEE Trans. Med. Imag. (TMI)*, vol. 43, no. 5, pp. 2021–2032, 2024.
- [23] J. Lee, D. Jung, J. Yim, and S. Yoon, "Confidence score for source-free unsupervised domain adaptation," in *Int. Conf. Mach. Learn. (ICML)*. PMLR, 2022, pp. 12 365–12 377.
- [24] J. H. A. Samadh, H. Gani, N. H. Hussein, M. U. Khattak, M. Naseer, F. Khan, and S. Khan, "Align your prompts: Test-time prompting with distribution alignment for zero-shot generalization," in *Proc. Adv. Neural Inform. Process. Syst. (NeurIPS)*, vol. 36, 2023, pp. 80 396–80 413.
- [25] S. Tang, Y. Shi, Z. Ma, J. Li, J. Lyu, Q. Li, and J. Zhang, "Model adaptation through hypothesis transfer with gradual knowledge distillation," in *Proc. IEEE/RSJ Int. Conf. Intell. Rob. Syst. (IROS)*. IEEE, 2021, pp. 5679–5685.
- [26] M. Shu, W. Nie, D.-A. Huang, Z. Yu, T. Goldstein, A. Anandkumar, and C. Xiao, "Test-time prompt tuning for zero-shot generalization in vision-language models," *Proc. Adv. Neural Inform. Process. Syst. (NeurIPS)*, vol. 35, pp. 14 274–14 289, 2022.
- [27] L. Chen, J. Li, X. Dong, P. Zhang, C. He, J. Wang, F. Zhao, and D. Lin, "ShareGPT4v: Improving large multi-modal models with better captions," in *Proc. Eur. Conf. Comput. Vis. (ECCV)*. Springer, 2024, pp. 370–387.
- [28] S. Tang, W. Su, M. Ye, and X. Zhu, "Source-free domain adaptation with frozen multimodal foundation model," in *Proc. IEEE Conf. Comput. Vis. Pattern Recog. (CVPR)*, 2024, pp. 23 711–23 720.
- [29] W. Zhang, L. Shen, and C.-S. Foo, "Source-free domain adaptation guided by vision and vision-language pre-training," *Int. J. Comput. Vis.*, vol. 133, no. 2, pp. 844–866, 2025.
- [30] D. Chen, K. Patwari, Z. Lai, S.-c. Cheung, and C.-N. Chuah, "Empowering source-free domain adaptation with mllm-driven curriculum learning," *arXiv preprint arXiv:2405.18376*, 2024.
- [31] S. Tang, W. Su, Y. Gan, M. Ye, J. Zhang, and X. Zhu, "Proxy denoising for source-free domain adaptation," in *Int. Conf. Learn. Represent. (ICLR)*, 2025, DOI: <https://arxiv.org/abs/2406.01658>.
- [32] B. Schölkopf, F. Locatello, S. Bauer, N. R. Ke, N. Kalchbrenner, A. Goyal, and Y. Bengio, "Toward causal representation learning," *Proceedings of the IEEE*, vol. 109, no. 5, pp. 612–634, 2021.
- [33] Y. Chen and P. Bühlmann, "Domain adaptation under structural causal models," *J. Mach. Learn. Resear. (JMLR)*, vol. 22, no. 1, pp. 11 856–11 935, 2021.
- [34] R. Christiansen, N. Pfister, M. E. Jakobsen, N. Gnecco, and J. Peters, "A causal framework for distribution generalization," *IEEE Trans. Pattern Anal. Mach. Intell.*, vol. 44, no. 10, pp. 6614–6630, 2021.
- [35] W. Wang, X. Lin, F. Feng, X. He, M. Lin, and T.-S. Chua, "Causal representation learning for out-of-distribution recommendation," in *Proc. ACM Web Conf. (WWW)*, 2022, pp. 3562–3571.
- [36] C. Ouyang, C. Chen, S. Li, Z. Li, C. Qin, W. Bai, and D. Rueckert, "Causality-inspired single-source domain generalization for medical image segmentation," *IEEE Trans. Med. Imag. (TMI)*, vol. 42, no. 4, pp. 1095–1106, 2022.
- [37] F. Lv, J. Liang, S. Li, B. Zang, C. H. Liu, Z. Wang, and D. Liu, "Causality inspired representation learning for domain generalization," in *Proc. IEEE Conf. Comput. Vis. Pattern Recog. (CVPR)*, 2022, pp. 8046–8056.
- [38] Z. Yue, Q. Sun, X.-S. Hua, and H. Zhang, "Transporting causal mechanisms for unsupervised domain adaptation," in *Proc. IEEE Int. Conf. Comput. Vis. (ICCV)*, 2021, pp. 8599–8608.
- [39] R. Wang, M. Yi, Z. Chen, and S. Zhu, "Out-of-distribution generalization with causal invariant transformations," in *Proc. IEEE Conf. Comput. Vis. Pattern Recog. (CVPR)*, 2022, pp. 375–385.
- [40] D. Mahajan, S. Tople, and A. Sharma, "Domain generalization using causal matching," in *Int. Conf. Mach. Learn. (ICML)*. PMLR, 2021, pp. 7313–7324.
- [41] J. Peters, D. Janzing, and B. Schölkopf, *Elements of causal inference: foundations and learning algorithms*. The MIT Press, 2017.
- [42] K. Zhou, J. Yang, C. C. Loy, and Z. Liu, "Learning to prompt for vision-language models," *Int. J. Comput. Vis.*, vol. 130, no. 9, pp. 2337–2348, 2022.
- [43] K. Kawaguchi, Z. Deng, X. Ji, and J. Huang, "How does information bottleneck help deep learning?" in *Proc. Int. Conf. Mach. Learn. (ICML)*. PMLR, 2023, p. 16049–16096.
- [44] N. Tishby, F. C. Pereira, and W. Bialek, "The information bottleneck method," *arXiv preprint physics/0004057*, 2000.
- [45] R. Houthoofd, X. Chen, Y. Duan, J. Schulman, F. De Turck, and P. Abbeel, "Vime: Variational information maximizing exploration," *Proc. Adv. Neural Inform. Process. Syst. (NeurIPS)*, vol. 29, 2016.
- [46] D. Barber and F. Agakov, "The im algorithm: a variational approach to information maximization," *Proc. Adv. Neural Inform. Process. Syst. (NeurIPS)*, vol. 16, no. 320, p. 201, 2004.
- [47] X. Ji, J. F. Henriques, and A. Vedaldi, "Invariant information clustering for unsupervised image classification and segmentation," in *Proc. IEEE Int. Conf. Comput. Vis. (ICCV)*, 2019, pp. 9865–9874.
- [48] B. Li, Y. Shen, Y. Wang, W. Zhu, D. Li, K. Keutzer, and H. Zhao, "Invariant information bottleneck for domain generalization," in *Proc. AAAI Conf. Artif. Intell. (AAAI)*, vol. 36, no. 7, 2022, pp. 7399–7407.
- [49] A. Krause, P. Perona, and R. Gomes, "Discriminative clustering by regularized information maximization," *Proc. Adv. Neural Inform. Process. Syst. (NeurIPS)*, vol. 23, 2010.
- [50] C. Ge, R. Huang, M. Xie, Z. Lai, S. Song, S. Li, and G. Huang, "Domain adaptation via prompt learning," *IEEE Transactions on Neural Networks and Learning Systems*, 2023.
- [51] Z. Lai, N. Vedapant, N. Zhou, J. Wu, C. P. Huynh, X. Li, K. K. Fu, and C.-N. Chuah, "PADCLIP: Pseudo-labeling with adaptive debiasing in clip for unsupervised domain adaptation," in *Proc. IEEE Int. Conf. Comput. Vis. (ICCV)*, 2023, pp. 16 155–16 165.
- [52] M. Singha, H. Pal, A. Jha, and B. Banerjee, "Ad-clip: Adapting domains in prompt space using clip," in *Proc. IEEE Int. Conf. Comput. Vis. (ICCV)*, 2023, pp. 4355–4364.

- [53] S. Yang, S. Jui, J. van de Weijer, *et al.*, “Attracting and dispersing: A simple approach for source-free domain adaptation,” *Proc. Adv. Neural Inform. Process. Syst. (NeurIPS)*, vol. 35, pp. 5802–5815, 2022.
- [54] D. Chen, D. Wang, T. Darrell, and S. Ebrahimi, “Contrastive test-time adaptation,” in *Proc. IEEE Conf. Comput. Vis. Pattern Recog. (CVPR)*, 2022, pp. 295–305.
- [55] S. Tang, A. Chang, F. Zhang, X. Zhu, M. Ye, and C. Zhang, “Source-free domain adaptation via target prediction distribution searching,” *Int. J. Comput. Vis.*, vol. 132, no. 3, pp. 654–672, 2024.
- [56] H. Venkateswara, J. Eusebio, S. Chakraborty, and S. Panchanathan, “Deep hashing network for unsupervised domain adaptation,” in *Proc. IEEE Conf. Comput. Vis. Pattern Recog. (CVPR)*, 2017, pp. 5385–5394.
- [57] X. Peng, B. Usman, N. Kaushik, J. Hoffman, D. Wang, and K. Saenko, “VisDA: The visual domain adaptation challenge,” *arXiv:1710.06924*, 2017.
- [58] X. Peng, Q. Bai, X. Xia, Z. Huang, K. Saenko, and B. Wang, “Moment matching for multi-source domain adaptation,” in *Proc. IEEE Int. Conf. Comput. Vis. (ICCV)*, 2019, pp. 1406–1415.
- [59] K. Han, Y. Wang, H. Chen, X. Chen, J. Guo, Z. Liu, Y. Tang, A. Xiao, C. Xu, Y. Xu, *et al.*, “A survey on vision transformer,” *IEEE Trans. Pattern Anal. Mach. Intell.*, vol. 45, no. 1, pp. 87–110, 2022.
- [60] J. Huang, D. Guan, A. Xiao, and S. Lu, “Model adaptation: Historical contrastive learning for unsupervised domain adaptation without source data,” *Proc. Adv. Neural Inform. Process. Syst. (NeurIPS)*, vol. 34, pp. 3635–3649, 2021.
- [61] K. Zhou, J. Yang, C. C. Loy, and Z. Liu, “Conditional prompt learning for vision-language models,” in *Proc. IEEE Conf. Comput. Vis. Pattern Recog. (CVPR)*, 2022, pp. 16816–16825.
- [62] B. Zhu, Y. Niu, Y. Han, Y. Wu, and H. Zhang, “Prompt-aligned gradient for prompt tuning,” in *Proc. IEEE Int. Conf. Comput. Vis. (ICCV)*, 2023, pp. 15 659–15 669.
- [63] B. Recht, R. Roelofs, L. Schmidt, and V. Shankar, “Do imagenet classifiers generalize to imagenet?” in *Int. Conf. Mach. Learn. (ICML)*. PMLR, 2019, pp. 5389–5400.
- [64] D. Hendrycks, K. Zhao, S. Basart, J. Steinhardt, and D. Song, “Natural adversarial examples,” in *Proc. IEEE Conf. Comput. Vis. Pattern Recog. (CVPR)*, 2021, pp. 15 262–15 271.
- [65] K. He, X. Zhang, S. Ren, and J. Sun, “Deep residual learning for image recognition,” in *Proc. IEEE Conf. Comput. Vis. Pattern Recog. (CVPR)*, 2016, pp. 770–778.
- [66] D. Hendrycks, S. Basart, N. Mu, S. Kadavath, F. Wang, E. Dorundo, R. Desai, T. Zhu, S. Parajuli, M. Guo, *et al.*, “The many faces of robustness: A critical analysis of out-of-distribution generalization,” in *Proc. IEEE Int. Conf. Comput. Vis. (ICCV)*, 2021, pp. 8340–8349.
- [67] H. Wang, S. Ge, Z. Lipton, and E. P. Xing, “Learning robust global representations by penalizing local predictive power,” *Proc. Adv. Neural Inform. Process. Syst. (NeurIPS)*, vol. 32, 2019.
- [68] M. Arjovsky, L. Bottou, I. Gulrajani, and D. Lopez-Paz, “Invariant risk minimization,” *arXiv preprint arXiv:2006.10726*, 2019.